A WIDE-FIELD K-BAND GALAXY SURVEY

J. P. Gardner[1], R. M. Sharples[2], C. M. Baugh[2], C. S. Frenk[2], & B. E. Carrasco[3]
[1] *NOAO/NASA/GSFC, Code 681, Greenbelt MD 20771, USA.*
[2] *University of Durham, Physics Dept., South Road, Durham DH1 3LE, UK.*
[3] *INAOE, Apdo Postal 216 y 51, Puebla, CP 72000, MEXICO.*

Abstract

We present the bright number counts, the luminosity function and the surface brightness distribution of the galaxies in a wide-field $K-$band selected galaxy redshift survey. We find that our galaxy count data are consistent with simple passive evolution of galaxies at $z < 0.3$, and we do not see the steep slope of the counts that has been seen in surveys done with photographic plates. The best-fit Schechter function parameters of the $K-$band galaxy luminosity function are $M^* = -23.12 + 5log(h)$, $\alpha = -0.91$, and $\phi^* = 1.66 \times 10^{-2} h^3\ Mpc^{-3}$. We estimate that systematics are no more than $0.1mag$ in M^* and 0.1 in α, which is comparable to the statistical errors on this measurement. We find a correlation between central surface brightness and redshift, but this is due primarily to a correlation between central surface brightness and absolute magnitude. We find that our redshift survey is not biased against low surface brightness galaxies because the V_{max} of every galaxy due to our apparent magnitude limit is smaller than the V_{max} of the galaxy due to our surface brightness limit.

1 Introduction

Observational studies of galaxy formation and evolution have advanced at an unprecedented pace in recent years. Two developments have played a key role: CCD imagery to very faint limits and the ability to measure redshifts for large samples at increasingly faint magnitudes. Progress to date has relied primarily on optical data, but it has been clear for some time that near-infrared observations are fundamental. Samples selected according to $K-$band flux are superior to the traditional $B-$selected samples in at least three respects: *(i)* In the infrared, K-corrections due to the redshift of the spectral energy distribution are smooth, well-understood, and nearly independent of Hubble type; the expected luminosity evolution is also smooth. *(ii)* At high redshift, the observer's near-infrared samples the well-understood rest frame optical

(dominated by long-lived, near-solar mass stars), while the optical band samples the poorly-understood rest frame ultraviolet (dominated by short-lived massive stars.) *(iii)* Since near-solar mass stars make up the bulk of a galaxy, the absolute K magnitude is a measure of the visible mass in a galaxy.

The luminosity function of galaxies is central to many problems in cosmology, including the interpretation of faint number counts. Because of this, the faint end slope of the luminosity function is currently the subject of much debate. Most measurements of the optical luminosity function of field galaxies show a flat slope, corresponding to $\alpha \approx -1.0$ in the Schechter (1976) parameterization (Efstathiou, Ellis & Peterson 1988; Loveday et al. 1992; Lin et al. 1996; but see Marzke et al. 1994). Deep field galaxy surveys, on the other hand, detect a very steep slope for the faint end of the optical number count relation, at the point where the relation could be dominated by the faint end slope of the local luminosity function (Tyson 1988; Lilly, Cowie & Gardner 1991; Metcalfe et al. 1996; but see also Cowie et al. 1996). In general, studies of galaxy evolution through number counts, colors, redshift distributions and clustering properties, all require an understanding of the local population of galaxies for interpretation of the faint end data.

2 Description of the Survey

We have imaged 9.84 square degrees in the $K-$band with a 256^2 HgCdTe NICMOS3 detector, and in the B, V, and I bands with a 2048^2 CCD camera. The $K-$band observations were made in 1994 June with the IRIM camera on the Kitt Peak National Observatory $1.3m$ telescope. On this telescope, the IRIM camera has $1.96''$ pixels and an $8.36'$ field of view. Each point was observed with at least two $60sec$ exposures, reaching a 5σ galaxy detection depth of $K = 15.6$ in a $10''$ circular aperture. The 3σ surface brightness limit of our images is $K = 18.5\ mag/\Box''$. The $B-$, $V-$, and $I-$band observations were made in 1995 June with the T2KA camera on the KPNO $0.9m$ telescope. On this telescope, the T2KA CCD has $0.68''$ pixels with a $23.2'$ field of view. Each point in each filter was observed with a $300sec$ exposure, and the images reach a 5σ detection depth of $B = 21.1$, $V = 20.9$, and $I = 19.6$ in a $10''$ circular aperture. The 3σ surface brightness limit is 24.0, 23.8, and 22.2 $mag/\Box''$ for B, V and I respectively. The location of the two fields were selected randomly, that is, without regard to the presence or absence of any known objects. The field centers are at RA 14^h15^m, Dec +00 and RA 18^h00^m, Dec +66; galactic latitudes +55 and +30 respectively. One of our fields has a nearby rich galaxy cluster within it, and to avoid biasing the galaxy counts, we have removed all objects within 1 degree radius of the central galaxy of this cluster. Thus the effective area for the counts presented here is 8.54 square degrees.

We have conducted a spectroscopic redshift survey of galaxies selected on the basis of their $K-$band flux in an area of approximately 4.4 square degrees, from within the larger photometric survey. In 1996 May, we used the $4.2m$ William Herschel Telescope on La Palma with the Autofib-2 fiber positioner and the WYFFOS spectrograph, to obtain spectra of 567 objects selected at $K < 15$. Approximately 75% of the spectroscopic observations were made in the NGP field, and the remainder were made in the NEP field (see Paper II). Objects within the photometric sample were selected for spectroscopy on purely geometrical criteria determined by the characteristics of Autofib-2. There is a small bias against interacting galaxies, since fibers could not be placed closer than $30''$ apart. The data reduction was done with the wyfred package written by Jim Lewis at the Royal Greenwich Observatory, and the redshift identification was done with software developed by Karl Glazebrook. We obtained good identifications and redshifts of 465 galaxies in the sample, and less certain redshifts for an additional 45 galaxies.

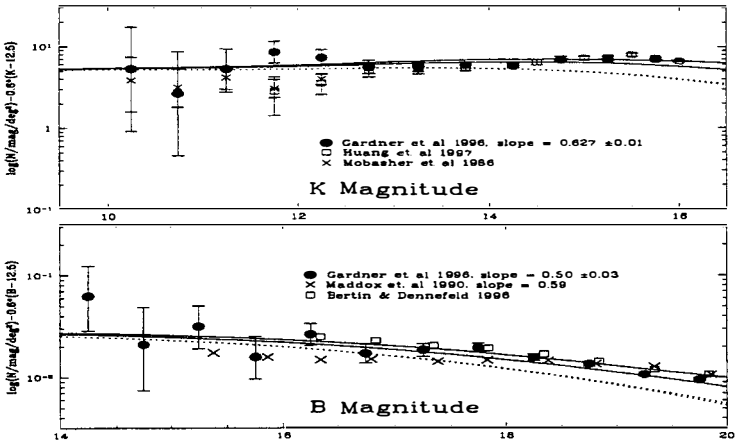

Figure 1: The $B-$ and $K-$band galaxy counts. The Euclidean slope, d $\log(n)/\mathrm{d}m$=0.6, has been subtracted in order to expand the ordinate. The models plotted are no-evolution (dotted line) and passive evolution (solid line), in an open universe (the two middle lines at faint magnitudes) and a closed universe. Our counts show a shallower slope than some other measurements, and are consistent with passive evolution models.

The latter have spectra with poor signal-to-noise, poor sky subtraction, or only a single significant line or break. Three objects were identified spectroscopically as stars. The remaining 54 galaxies were unidentified, giving a completeness of 90%. We have presented the galaxy counts in Gardner et al. (1996) (Paper I), the clustering properties in Baugh et al. (1996) (Paper II), and the $K-$band luminosity function of galaxies in Gardner et al. (1997) (Paper III).

3 Galaxy Counts

The $B-$band and $K-$band galaxy number counts are plotted in Figure 1. To expand the ordinate, we have subtracted the Euclidean slope $dlog(n)/dm = 0.6$. Alongside our data, we plot other existing bright galaxy counts. For comparison we also show the predictions of a simple model, based upon the formulation of Yoshii & Takahara (1988), modified to include rest-frame and evolved spectral energy distributions from the GISSEL models (Bruzual & Charlot 1993; 1997 in preparation.) The model is similar to that used in Gardner (1996), except that we have used the revised version of the GISSEL models. The solid lines include this passive evolution, while the dotted lines are no-evolution models, i.e. models that include only the cosmological geometry and K-corrections. To constuct the models we adopted the b_J type-independent luminosity function of Loveday et al. (1992), converted to type-dependent luminosity functions in other filters through rest frame colours. The normalization of the models was determined with a least-squares fit of the passive-evolution flat universe model to our data.

Our counts in the region $13 < K < 15$ are within 1σ of the Huang et al. (1996) counts in each magnitude bin, which were also based upon $K-$band observations of approximately 10

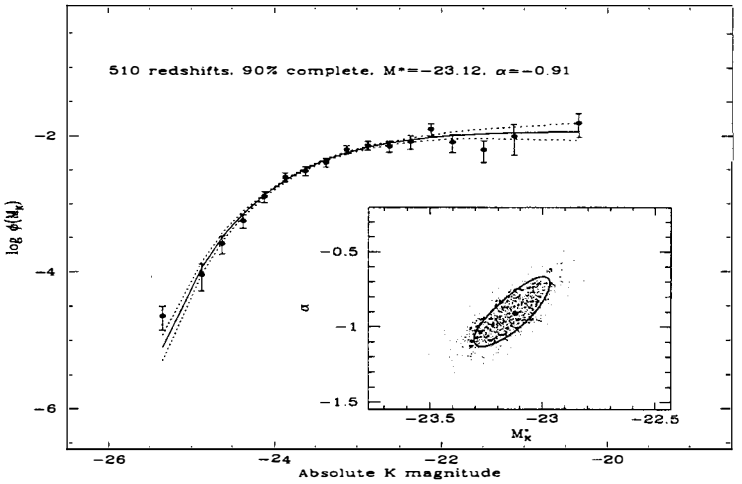

Figure 2: The differential $K-$band luminosity function of galaxies. The points and their errors were determined from our data using the SWML method of EEP. The solid line is the best fit Schechter function determined using the STY maximum likelihood method. The dashed lines show the effect of varying the parameters of the fit by $\pm 1\sigma$, as determined from the error ellipse. Inset are the error ellipse on the Schechter parameter fit to the luminosity function, and the results of 1000 Monte Carlo simulations of our survey parameters. These simulations were binned as 0.03 in M^* and 0.03 in α, and a contour containing 68% (i.e. 1σ) of the points in the binned data is shown as a dashed line.

square degrees. The consistency of the two results indicates that both surveys represent a fair sample of the universe, so the bright $K-$band galaxy counts and their normalization are no longer a subject of debate. Nevertheless, we measure a shallower slope. The slope of our counts is 0.627 ± 0.010, consistent with the flat-universe passive evolution model plotted in Figure 1. Thus our data do not support the conclusion of Huang et al. (1996) that a model with a steep slope is required to fit the bright $K-$band number counts.

The $B-$band galaxy counts are also plotted in Figure 1. We used the Kitt Peak standard B filter, corrected to the Johnson B standard stars of Landolt, (1983; 1992). The B counts have been measured in many surveys, but this is the first time that B counts at $B < 20$ have been obtained with a CCD camera, rather than with non-linear photographic plates. While our area is much smaller than other surveys, and our statistical error is higher, our counts are far less likely to suffer from systematic effects in the photometry. In Figure 1 we have plotted b_J counts, converted to the Johnson $B-$band, from the APM survey of Maddox et al. (1990) (hereafter APM), and from the MAMA survey of Bertin & Dennefeld (1997).

The APM counts show the steep slope at the bright end mentioned earlier. These authors interpretated the data as revealing a large (and unexpected) amount of luminosity evolution at low redshifts ($z < 0.1$). Other workers have attributed this steep slope to a local underdensity of galaxies (Shanks 1990; Metcalfe et al. 1991), to a selection effect against low surface brightness galaxies (McGaugh 1994; Ferguson & McGaugh 1995), or to systematics in the photometry

(Metcalfe, Fong & Shanks 1995). The slope measured in the APM data at $16 < B < 19$ is 0.59, while a linear fit to our data in this same range of magnitudes gives a slope of 0.50 ± 0.03. Our measured slope is consistent with passive evolution models, which have slopes of 0.52 and 0.51 for $q_0 = 0.5$ and 0 respectively, and agrees with that of Bertin & Dennefeld (1997), who surveyed 145 square degrees using individually calibrated Schmidt plates. We have normalized the flat-universe passive-evolution model with a least-squares fit to our data. This normalization is equivalent to using a Schechter luminosity function with $b_J^* = -19.50 + 5log(h)$ and $\alpha = -0.97$, as measured by Loveday et al. (1992), but with $\phi^* = 2.02 \times 10^{-2} h^3 Mpc^{-3}$, a normalization that is a factor of 1.44 times higher than that measured in the Stromlo-APM survey (Loveday et al. 1992.) High normalization models have been proposed to reduce the excess of faint blue galaxies that has been seen in deep photometric surveys (for a review, see Ellis 1997), and to fit the WFPC2 Medium Deep Survey results (Glazebrook et al. 1995; Driver et al. 1995).

4 The K−band Luminosity Function of Galaxies

We calculated the luminosity function from our data using the SWML method (Efstathiou et al. 1988). The results are plotted in Figure 2. We determined the variances using the constraint given by Efstathiou et al. (1988), with $M_{fid} = -23.5 + 5log(h)$ and $\beta = 1.5$, where $H_0 = 100h\ km\ s^{-1}\ Mpc^{-1}$. We used the maximum likelihood method of Sandage, Tammann & Yahil (1979) to determine the best fit Schechter function parameters, $M^* = -23.12 + 5log(h)$, and $\alpha = -0.91$, and this function is plotted as a solid line in Figure 2, with the error ellipse in M^* and α plotted in the inset. We used a number count model fit to our measured counts to determine the normalization $\phi^* = 1.66 \times 10^{-2} h^{-3}\ Mpc^{-3}$. The dashed lines on either side of the Schechter function in Figure 2 show the effect of varying M^* and α by $\pm 1\sigma$. As a check of our error determinations, we ran 1000 Monte Carlo simulations of the survey. Using a number count model, we assigned redshifts and absolute magnitudes to a mock sample of 510 galaxies selected at $K < 15$, and we determined the Schechter parameters using the maximum likelihood method. These 1000 simulations are plotted in the inset to Figure 2. The contour enclosing 68% of the points agrees approximately with the error ellipse determined from the likelihood. The mean parameter values from the 1000 simulations differed from the inputs by $-0.03 mag$ in M^*, and -0.01 in α, and this may be taken as an indication of systematic errors in the techniques used, and of the inaccuracy in the number count model. We used a similar Monte Carlo technique to look for systematic effects due to photometric errors, and due to the fraction of identified galaxies as a function of magnitude. We used a two sample Kolmogorov-Smirnov test to determine whether the identified and unidentified galaxies were drawn from the same population in color and surface brightness. These tests showed that the systematic errors are less than $0.1 mag$ in M^* and 0.1 in α, which is comparable to the statistical errors of our luminosity function measurement (Gardner et al. 1997).

5 Surface Brightness Effects

Attempts to measure the rest-frame surface brightness distribution of galaxies have produced divergent results. In an early study of 36 spiral and S0 galaxies, Freeman (1970) concluded that the galaxies have a preferred central surface brightness, but Disney (1976) claimed that this is a selection effect due to the surface brightness detection limits of photographic plates and the brightness of the night sky. This debate has continued to the present day, but it can be summarized as follows. Photometric surveys have two limits. They reach a limiting apparent

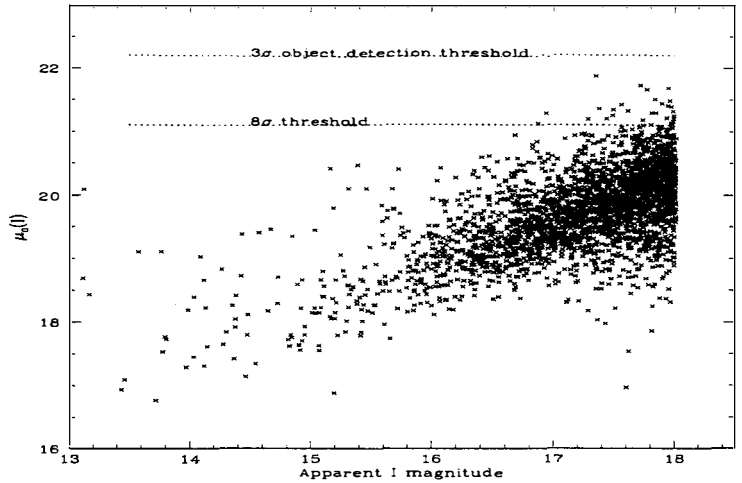

Figure 3: Central surface brightness measured by fitting an exponential to the radial profile of galaxies in the $I-$band, $\mu_0(I)$. plotted against apparent I magnitude. Galaxies with near neighbors have been removed. There is a clear trend to lower central surface brightness at fainter magnitudes, which is caused mainly by the $(1+z)^4$ cosmological dimming. Our nominal 3σ object detection limit is shown, along with a much more conservative 8σ limit.

magnitude, and reach a limiting surface brightness threshold. Whether a bias is introduced by the distribution of surface brightness of galaxies will depend upon the interpretation, and whether the apparent magnitude limit is a stronger constraint on the observations than the surface brightness limit.

The radial profiles of spiral galaxies are commonly assumed to follow an exponential, $\mu \propto \mu_0 + 1.086(r/\alpha)$, while elliptical galaxies are assumed to follow $\mu \propto \mu_0 + 8.325[(r/r_0)^{1/4} - 1]$ (Kormendy 1977). Galaxies often show characteristics of both, with a sperical bulge and a spiral disk. Observationally, these profiles will be convolved with the seeing.

The resolution, depth and pixel size of our optical images was much better than our $K-$band images, so object selection and $K-$band photometry was done by identifying objects on our $I-$band images, using the SExtractor package (Bertin & Arnouts 1996), and putting a $10''$ aperture on that position on our $K-$band images. On the assumption that there is no dependence of $I-K$ color on radius of the galaxy, the resulting flux was corrected to a total magnitude by adding the difference between the SExtractor $I-$band *mag_best* and the $I-$band flux in a $10''$ aperture. When galaxies overlapped, the $K-$band aperture magnitudes were deblended individually by assigning entire pixels to the individual galaxies. Because the initial galaxy detection was done with the optical images, we must examine the $I-$band surface brightness distribution of our sample for any potential surface brightness selection effects. However, if we are concerned with completeness in our $K-$band selected redshift sample, it is only necessary to establish that any selection effects that we find do not affect the redshift survey.

We measured the central surface brightness of all of our objects by fitting an exponential profile to the radial profile. We expanded the images by a factor of eight in each direction,

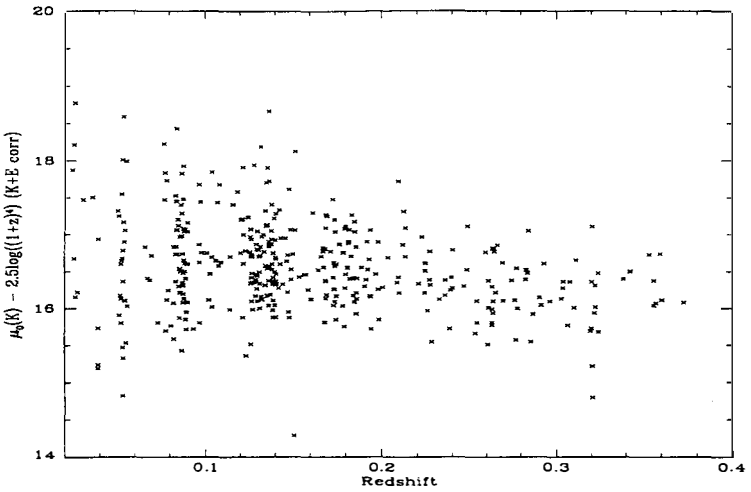

Figure 4: Rest-frame central surface brightness of isolated galaxies in the K band, obtained by subtracting a small aperture $I - K$ color from the measured $\mu_0(I)$, and correcting for the cosmological dimming and K– and E–corrections.

and we calculated the radial profile within a 15″ diameter aperture. This fully automatic process is subject to some uncertainty, which we consider below. Figure 3 is a plot of the central surface brightness $\mu_0(I)$ against apparent I magnitude, for our $I < 18$ galaxy sample. Objects having near neighbors or requiring deblending have been removed. Our object detection algorithm began by classifying any pixel having a flux higher than 3σ or $\mu(I) < 22.2\ mag/\square''$ as a potential object. We then attempted to measure the magnitude of the object to determine whether or not it fell within our survey limits. Star/galaxy separation and the removal of cosmic ray hits from our catalog is discussed in detail in Paper V (Gardner et al., in preparation), but one aspect deserves mention here. As part of the process, we examined on a contour plot any object which we suspected to be a cosmic ray, or for which the color star/galaxy separation criterion disagreed with the morphological criterion (based on a Kron r_{-2} measurement, Kron 1980). These contour plots were made with the lowest contour at 2σ per pixel, and with each successive contour twice the level of the previous one. Objects which looked very compact or which contained only one or two contours were identified as cosmic ray hits, either in the optical band, or in the K–band. Thus is it possible that a low-surface brightness object appearing just over the detection threshold would have looked compact on the contour plots and been identified as a cosmic ray. In our analysis we will examing our catalog for selection effects using two surface brightness thresholds, our nominal object identification threshold of 3σ, and a very conservative threshold of 8σ, or $\mu_0(I) = 21.1\ mag/\square''$, corresponding to 3 contours on the contour plots.

Selection effects in galaxy surveys at low to intermediate redshift due to the surface brightness distribution of galaxies take at least two forms. When the central surface brightness of a galaxy is fainter than the limiting threshold used for object detection, the galaxy will not be identified Ferguson & McGaugh (1995). The central surface brightness of a galaxy depends

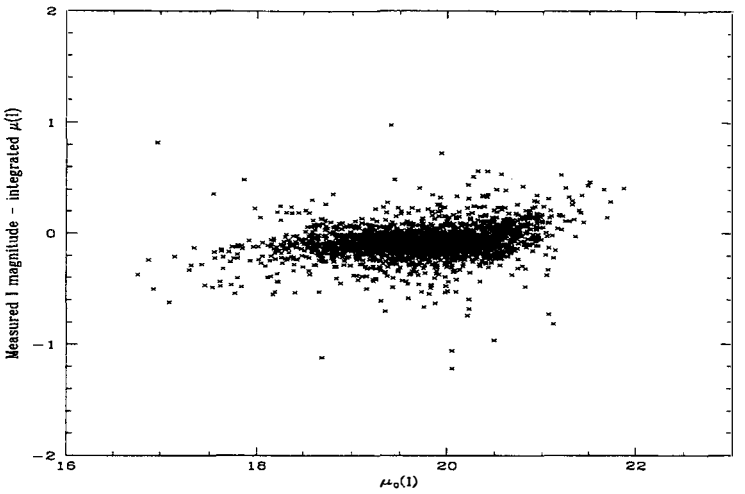

Figure 5: Dependence of measured magnitude on surface brightness. We have integrated our measurement of the exponential profile of the galaxies (an estimate of total magnitude), and subtracted this from our measured magnitude. The data are consistent with a small offset from total magnitude, although there is a slight turnup at lowcentral surface brightness, and a turndown at high central surface brightness.

on redshift through cosmological dimming $\propto (1+z)^4$, and through K–corrections and passive evolution. In Figure 4 we plot $\mu_0(K)$, (obtained by subtracting the $I-K$ color from $\mu_0(I)$, and correcting for cosmological dimming, K–, and E–corrections,) against redshift for our $K < 15$ spectroscopic sample. While there is a wide distribution in observed surface brightness at low redshift, we do not see low surface brightness galaxies at our high redshift limit. This, however, is not necessarily due to surface brightness selection effects, it could be due to our apparent magnitude limit. For each galaxy in our $K < 15$ spectroscopic survey, we calculated V_{max}, the volume in which the galaxy would have been observed within the selection effects of the survey. For every galaxy, V_{max} determined from our apparent magnitude limit is larger than V_{max} determined from our 8σ surface brightness limit, when corrected for the effects of cosmological dimming, K–, and E– corrections. The objects for our spectroscopic survey were selected from images which were sufficiently deep relative to our selection limit that results that depend upon the apparent magnitude limit, such as the luminosity function reported in Paper III, are not affected by the surface brightness of the galaxies.

Surface brightness has another, more subtle effect on the selection function for galaxies. McGaugh (1994) has shown that isophotal magnitudes show a dependence on surface brightness, in which the photometry of low surface brightness galaxies is systematically underestimated. If there is a large population of galaxies showing this effect, then the number counts would be higher than the measurements, and the faint-end slope of the luminosity function would be steeper than the measurements. In our survey, we did the optical photometry with the SExtractor *mag_best*, which is measured in an elliptical aperture at 2.5 times the Kron r_{-1} radius (Kron 1980) for isolated objects, and deblended isophotal magnitudes for objects with

close neighbors. As mentioned above, we measured the $K-$band magnitudes in a circular aperture which we corrected to total using the $I-$band image. This technique avoids many of the problems associated with isophotal magnitudes for isolated objects, and confusion was not a large problem in this wide-field survey.

Integrating an exponential profile gives $\mu_0 - 2.5log(2\pi\alpha^2)$. Figure 5 is a plot of our measured Kron magnitudes minus the integrated exponential fit ($I - \int \mu(I)$) against central surface brightness for our $I < 18$ isolated galaxy sample. For most galaxies, $I - \int \mu(I)$ is approximately zero, the median of the sample is -0.08, and the average is -0.035. There is an apparent turnup at the faint, as is expected from a systematic effect on the magnitudes due to surface brightness effects. However, there is also a turndown at the bright end, and both of these would be expected from inaccuracies in the fit of the exponential profiles.

6 Conclusions

We have conducted a photometric survey of 10 square degrees of the extragalactic sky in the K, I, V and B bands, and spectroscopic redshift survey of more than 500 galaxies selected at $K < 15$. Our galaxy counts are consistent with simple passive luminosity evolution of galaxies at low redshift, and we do not see the steep slope of the bright counts that has been seen in other surveys. We have measured the $K-$band luminosity function of galaxies, and determined that our measurement is not biased due to photometric errors, incompleteness, or the surface brightness distribution of galaxies.

References

[1] Baugh, C. M., Gardner, J. P., Frenk, C. S., & Sharples, R. M. 1996, MNRAS, 283, L15, (Paper II)

[2] Bertin, E., & Arnouts, S. 1996, A&AS, 117, 393

[3] Bertin, E., & Dennefeld, M. 1997, A&A, 317, 43

[4] Bruzual A., G., & Charlot, S. 1993, ApJ, 405, 538

[5] Cowie, L. L., Songaila, A., Hu, E. M. & Cohen, J. G. 1996, AJ, 112, 839

[6] Disney, M. J. 1976, Nature, 263, 573

[7] Driver, S. P., Windhorst, R. A., & Griffiths, R. E. 1995, ApJ453, 48

[8] Efstathiou, G., Ellis, R. S., & Peterson, B. A. 1988, MNRAS, 232, 431

[9] Ellis, R. S. 1997, ARA&A, 35, in press

[10] Ferguson, H. C., & McGaugh, S. S. 1995, ApJ, 440, 470

[11] Freeman, K. C. 1970, ApJ, 160, 811

[12] Gardner, J. P. 1996, MNRAS, 279, 1157

[13] Gardner, J. P., Sharples, R. M., Carrasco, B. E., & Frenk, C. S. 1996, MNRAS, 282, L1, (Paper I)

[14] Gardner, J. P., Sharples, R. M., Frenk, C. S., & Carrasco, B. E. 1997, ApJ, 480, L99, (Paper III)

[15] Glazebrook, K., Ellis, R., Santiago, B., & Griffiths, R. 1995, MNRAS, 275, L19

[16] Huang, J.-S., Cowie, L. L., Gardner, J. P., Hu, E. M., Songaila, A., & Wainscoat, R. J. 1997, ApJ, 476, 12

[17] Kormendy, J., 1977, ApJ, 217, 406
[18] Kron, R. G. 1980, ApJS, 43, 305
[19] Lilly, S. J., Cowie, L. L., & Gardner, J. P. 1991, ApJ, 369, 79
[20] Lin, H., Kirshner, R. P., Shectman, S. A., Landy, S. D., Oemler, A., Tucker, D. L., & Schechter, P. L. 1996, ApJ, 464, 60
[21] Loveday, J., Peterson, B.A., Efstathiou, G., & Maddox, S.J. 1992, ApJ, 390, 338
[22] Maddox, S. J., Sutherland, W. J., Efstathiou, G., Loveday, J., & Peterson, B. A. 1990, MNRAS, 247, 1P
[23] Marzke, R. O., Huchra, J. P. & Geller, M. J. 1994, ApJ, 428, 43
[24] McGaugh, S. S. 1994, Nature, 367, 538
[25] Metcalfe, N., Shanks, T., Fong, R., & Jones, L. R. 1991, MNRAS, 249, 498
[26] Metcalfe, N., Fong, R., & Shanks, T. 1995, MNRAS, 274, 769
[27] Metcalfe, N., Shanks, T., Campos, A., Fong, R., & Gardner, J. P. 1996, Nature, 383, 236
[28] Sandage, A., Tammann, G. A., & Yahil, A., 1979, ApJ, 232, 352
[29] Schechter, P. 1976, ApJ, 203, 297
[30] Shanks, T. 1990, in Bowyer, S., Leinert C., eds., Proc. IAU Symp. 139, The Galactic and Extragalactic Background Radiation, Kluwer, Dordrecht, p. 269
[31] Tyson, J. A. 1988, AJ, 96, 1
[32] Yoshii, Y., & Takahara, F. 1988, ApJ, 326, 1